Modelling of progressive short waves using wave envelopes

Edmund Chadwick
and Peter Bettess

School of Engineering, University of Durham
Science Laboratories, South Road
Durham DH1 3LE, England

March 1995
Revised November 1996

SUMMARY

We consider progressive waves such that the time independent potential satisfies the Helmholtz equation, for example, the travelling wave diffracted from a body. In order to model the wave potential using finite elements it is usual to discretize the domain such that there are about ten nodal points per wavelength. However, such a procedure is computationally expensive and impractical if the waves are short. The goal is to be able to model accurately with few elements problems such as sonar and radar. Therefore we seek a new method in which the discretization of the domain is more economical. To do so, we express the complex potential ϕ in terms of the real wave envelope A and the real phase p such that $\phi = Ae^{ip}$, and expect that in most regions the functions A and p vary much more gradually over the domain than does the oscillatory potential ϕ. Therefore instead of modelling the potential we model the wave envelope and the phase.

The usual approach then uses the well known geometrical optics approximation [1, p109]: if the wave number k is large then the potential can be expanded in decreasing powers of k. The first two terms give the eikonal equation for the phase and the transport equation for the wave envelope respectively [2, p149]. However, using the geometrical optics approximation (or

ray theory) gives no diffraction effects. This approach shall therefore not be considered. (We note though that Keller's theory of geometrical diffraction [3], an extension to geometrical optics, does allow for diffraction effects and this may be considered at a later date.)

We shall consider a new method which shall be described in the present paper and apply it to two dimensional problems, although the method is equally valid for arbitary three dimensional problems. (The method has already been validated for the case of one dimensional problems [4].) An iterative procedure is described whereby an estimate of the phase is first given and from the resulting finite element calculation for the wave envelope a better estimate for the phase is obtained. The iterated values for the phase and wave envelope converge to the expected values for the test progressive wave examples considered. Even if a very poor estimate for the phase is first given the iterated values converge to the exact values but very slowly.

1 Introduction

One way of modelling the wave envelope is to use a shape function which incorporates the harmonic variation of the potential. This idea was first introduced by Bettess and Zienkiewicz [5] [6]. However they adopted a Galerkin weighting. Although this leads to a symmetrical (complex) element matrix, it also generates non standard integrals over the element domain, for which special formulas were developed. Astley [7] [8] [9] later introduced the further innovation of a complex conjugate weighting, which reduces the integrals to a much simpler form, which can be evaluated using Gauss-Legendre integration. This is at the expense of Hermitian matrices, and also in unbounded problems, some line integrals arise at infinity. (The Hermitian matrix formulation implies that if the wave envelope of the geometrical optics approximation were to be determined a skew symmetric stiffnes matrix would be obtained. However, from [10, p31] (see also appendix A) skew symmetric matrices of odd order have zero determinant. This means that only an even number of unconstrained nodes can be considered.) Bettess and Chadwick [4] show that Astley is essentially modelling the wave envelope A in the far field where the phase p is known (the potential ϕ of a travelling wave is expressed in the form $\phi = Ae^{ip}$). In the present paper we model near field diffraction problems where the phase p is unknown. We note that the wave envelope A and phase p vary much more gradually over the domain than the potential

ϕ. Hence if we can model A and p rather than the potential then a coarser mesh (fewer nodes) can be used. However, we now have two real variables, A and p, to be determined rather than the single complex variable ϕ.

We consider an iterative method whereby an estimate of the phase p_0 is first given and from the resulting finite element calculation for the wave envelope A_0 a better estimate p_1 for the phase is obtained: since p_0 is an estimate for the phase p, we expect A_0 to have an imaginary part. Hence we consider a function β_0 such that

$$A_0 = |A_0|e^{i\beta_0} \tag{1}$$

and the first estimate for the potential ϕ_0 is given by

$$\phi_0 = A_0 e^{ip_0} = |A_0|e^{i(p_0+\beta_0)} \tag{2}$$

Hence we consider a better estimate for the phase p_1 to be

$$p_1 = p_0 + \beta_0 \tag{3}$$

and so the gradient vector change of the phase at the Gaussian points is given by

$$\underline{\nabla p_1} - \underline{\nabla p_0} = \underline{\nabla \beta_0} \tag{4}$$

where $\underline{\nabla}$ is the gradient operator $(\frac{\partial}{\partial x}, \frac{\partial}{\partial y})$ in (x, y) 2-D cartesian coordinates. Hence the Gauss-Legendre calculation with the new guess p_1 for the element integral can be obtained from (4). (We note that in our formulation, which involves an integration by parts of the element matrix integral, the second order change of the phase is not considered.) The iteration is repeated until β_0 (and therefore $\underline{\nabla \beta_0}$) becomes negligible.

We consider plane waves, the 2-D Helmholtz source and the diffraction potential from a vertical cylinder as test progressive waves for the method. All the tests of the method have proved to be successful. Even when the initial estimate is ten to twenty percent different from the actual value, the exact results are obtained after two or three iterations for a nodal spacing of one wavelength.

2 Method

We derive the Helmholtz equation for the potential ϕ from the time dependent wave equation for the time dependent potential Φ. We then substitute for $\phi = Ae^{ip}$ into the Helmholtz equation to obtain a second order differential equation in A and p. Since we provide an estimate for the phase, the wave envelope is the unknown to be determined from this expression using the finite element numerical computation. Hence we provide the finite element governing equation [11, p215] in the form of an integral expression of the wave envelope in the usual way (i.e. using the standard Galerkin shape and weighting functions [11, p215]). However, we can integrate by parts this integral and obtain a stiffness matrix which is hermitian. This shall be called the complete formulation. Further, we may assume, like Astley does for his far field elements, that the eikonal equation [2, p149] holds. This assumption reduces the terms in the element matrix integrand and shall be called the 'generalized Astley formulation'. The two formulations are given and in the results section compared against each other. We now derive the Helmholtz equation.

The time dependent wave equation [12, p493] is given by

$$\frac{\partial^2 \Phi}{\partial t^2} = c^2 \nabla^2 \Phi \tag{5}$$

for the time dependent wave potential $\Phi(x, y, t)$ where (x, y) are the two-dimensional cartesian coordinates, t is time, c is a constant defined as the wave speed and ∇^2 is the Laplacian operator. We look for a progressive wave solution of the form

$$\Phi = Re\{Ae^{i(ks-\omega t)}\} = A\cos(ks - \omega t) \tag{6}$$

where ω is the source frequency, A is the wave envelope and $p = ks$ is the phase. A and p are real. Hence the time independent wave potential

$$\phi = Ae^{ip} = Ae^{iks} \tag{7}$$

is complex for a progressive wave solution. Substituting (6) into (5) gives the Helmholtz potential

$$(\nabla^2 + k^2)\phi = 0 \tag{8}$$

where $k = \omega/c$ is the wavenumber. Further, substituting the wave envelope and the phase given by (7) into the Helmholtz equation (8) gives

$$k^2 A\{1 - \underline{\nabla s}.\underline{\nabla s}\} + ik\{2\underline{\nabla A}.\underline{\nabla s} + A\nabla^2 s\} + \nabla^2 A = 0 \tag{9}$$

where $\underline{\nabla}$ is the gradient vector operator $(\frac{\partial}{\partial x}, \frac{\partial}{\partial y})$.

For large k, the first order term gives the eikonal equation $\underline{\nabla s}.\underline{\nabla s} \sim 1$, and the second term gives the wave envelope from the transport equation $2\underline{\nabla A}.\underline{\nabla s} + A\nabla^2 s \sim 0$ [13, p88].]

We use the standard Galerkin finite element scheme [11, p215] to model the wave envelope A and so

$$\begin{aligned}\sum_i \int\int_D [k^2 N_j N_i\{1 - \underline{\nabla s}.\underline{\nabla s}\} + ikN_j\{2\underline{\nabla N_i}.\underline{\nabla s} + N_i\nabla^2 s\} \\ -\underline{\nabla N_j}.\underline{\nabla N_i}]dxdya_i = 0_j\end{aligned} \tag{10}$$

gives the governing finite element integral equations for the problem, where $A \sim \sum_i N_i a_i$ is the approximation for A used, N_i are the standard Galerkin shape functions and D is the domain. Thus a_i is the numerical approximation for A at node i and i is summed over all nodes. However, consider the following integration by parts

$$\begin{aligned}\int_C N_j N_i \underline{\nabla s}.\underline{n}dl &= \int\int_D \underline{\nabla}.(N_j N_i \underline{\nabla s})dxdy \\ &= \int\int_D \{N_j \underline{\nabla N_i}.\underline{\nabla s} + N_i \underline{\nabla N_j}.\underline{\nabla s} + N_j N_i \nabla^2 s\}dxdy\end{aligned} \tag{11}$$

where dl is an element of length along the boundary contour C which encloses the domain and $\underline{n}$ is the outward pointing normal vector to the contour. On the contour all the N_j, the weighting functions, are zero; the j equations are determined only at the unconstrained nodes. Thus there are the same number of equations in (11) as there are unknown values of a_j. Therefore $\int_C(N_j N_i \underline{\nabla s}.\underline{n})dl = 0_{ji}$. (We note that if an infinite domain is considered, and so the contour radius R tends to infinity, then in the limit this integral may return a constant value since $\int_C dl \sim 0(R)$, $\underline{\nabla s} \sim 0(1)$, $N_j N_i \sim 0(\frac{1}{R})$. See Bettess [14, p214-215]. However, in the present paper we shall consider only finite domains.) Thus substituting (11) into (10) gives

$$\begin{aligned}\sum_i \int\int_D [k^2 N_j N_i\{1 - \underline{\nabla s}.\underline{\nabla s}\} + ik\{N_j \underline{\nabla N_i}.\underline{\nabla s} - N_i \underline{\nabla N_j}.\underline{\nabla s}\} \\ -\underline{\nabla N_j}.\underline{\nabla N_i}]dxdya_i = 0_j.\end{aligned} \tag{12}$$

We shall call this the 'complete formulation' since the eikonal equation assumption has not been made. The stiffness matrix $k_{ij}^{(1)}$ for the complete formulation is therefore given by

$$k_{ij}^{(1)} = \int\int_D [k^2 N_j N_i\{1 - \underline{\nabla s}.\underline{\nabla s}\} + ik\{N_j \underline{\nabla N_i}.\underline{\nabla s} - N_i \underline{\nabla N_j}.\underline{\nabla s}\} \\ - \underline{\nabla N_j}.\underline{\nabla N_i}]dxdy \qquad (13)$$

(The matrix equation is $k_{ij}^{(1)} a_i = 0_j$.) The formulation has the same attributes as the Astley wave envelope formulations in that (a) the matrix is hermitian and (b) the element matrix is given in terms of the phase gradient $\underline{\nabla s}$ rather than also including second order changes in the term $\nabla^2 s$. If the eikonal equation is assumed valid, which Astley correctly assumes in the far field [7] [8] [9], then we obtain the stiffness matrix $k_{ij}^{(2)}$ such that

$$k_{ij}^{(2)} = \int\int_D \{-\underline{\nabla N_j}.\underline{\nabla N_i}\} + ik\{N_j \underline{\nabla N_i}.\underline{\nabla s} - N_i \underline{\nabla N_j}.\underline{\nabla s}\}dxdy \qquad (14)$$

We note that for large k (14) approximates to a skew symmetric matrix. We now show how a better estimate for the phase is determined from the previous value.

2.1 A new estimate for the phase function

Let the potential determined using the estimate $p_0 = ks_0$ for the phase function be ϕ_0. (The phase function is given at the nodes and interpolated from the nodal values by using the element shape functions.) We consider a new estimate ks_1 for the phase such that the potential ϕ_0 satisfies

$$\phi_0 = A_0 e^{iks_0} = |A_0| e^{i(ks_0 + \beta_0)} = |A_0| e^{iks_1} \qquad (15)$$

where $|A_0|$ is real (the modulus of A_0).In general the wave envelope A_0 will have an imaginary part. Hence ks_1 shall be used as the new estimate for the phase function such that

$$s_1 = s_0 - \frac{i}{k} \ln \left\{ \frac{A_0}{|A_0|} \right\} \qquad (16)$$

Hence the error in s_0 at node n is given by $\beta_0^n = \frac{1}{k} Im\{\ln A_0^n\}$ where A_0^n is the wave envelope at node n calculated from the f.e. stiffness matrix equation. We evaluate the element matrix integral by using the Gauss-Legendre approximation [14, p184]. The new estimate for the phase gradient which is $\underline{\nabla s_1}$ can therefore be calculated at the Gaussian points by

$$\underline{\nabla s_1} = \underline{\nabla s_0} + \frac{1}{k}\underline{\nabla \beta_0} \tag{17}$$

Hence the gradient of s is stored at each iteration and the 'error' added to it after the wave envelope is determined.

Hence an iteration procedure occurs and is stopped after m iterations when the imaginary part of A_m is negligible. Thus it is hoped that the iteration procedure converges to the actual values for the wave envelope and phase function. For the particular test examples considered, this is found to be the case. The test examples considered are given next

2.2 Test examples.

First, we consider the plane wave potential

$$\phi = e^{ikx} \ , \quad A = 1 \ , \quad s = x. \tag{18}$$

which we call example 1. Second, we consider the 2-D wave Hankel source [15, p358] (Hankel function of order zero)

$$\phi = H_0(kr) \ , r = \sqrt{x^2 + y^2} \tag{19}$$

which we call example 2. Lastly, we consider the wave elevation diffraction potential given by MacCamay and Fuchs [16] as a Bessel function expansion, using the result of Havelock [17]. In particular, we consider the potential given by

$$\phi = \phi_D = -H_0(kr)\frac{J_0'(ka)}{H_0'(ka)} - \sum_{n=1}^{\infty} 2i^n \frac{J_n'(ka)}{H_n'(ka)} H_n(kr) \cos n\theta \tag{20}$$

with cylinder radius $a = 1$ which we call example 3. (We note that the differential equation for this potential is not derived from (5) but from separation of variables of the z-coordinate in the Laplace equation. The results are now given.

3 Results

We shall first test the iteration method (using the complete formulation) on the plane wave and Hankel source; the estimate for s will be such that some unconstrained nodes (nodes within the domain) are perturbed from the exact value (By exact for examples 2 and 3 we mean the numerical evaluation of the phase from (19) and (20) respectively, which involve Bessel functions. The potential at the boundary is assumed known and hence the boundary nodes are constrained. The wave envelope and phase can be determined from the potential at the boundary and the algorithm used is described in the appendix B. A rectangular domain shall be considered.

We shall then compare and contrast the 'complete' and 'generalised Astley' formulations for the diffraction potential given by the Bessel summation (20). The estimate for s will be determined by assuming a linear variation in s throughout the domain. A cylinder-based domain shall be considered. First, we test the iteration method.

3.1 Testing the iteration method.

We consider a rectangular 5*5 grid of 25 evenly spaced nodes in the region $10 \leq x, y \leq 14$, such that the nodes on the rectangle circumference are constrained. The exact value of the phase is given at all nodes except 12, 13 and 14 where the phase value is perturbed by some fixed amount. The nodes are numbered row by row from the bottom left hand corner $x = y = 10$.

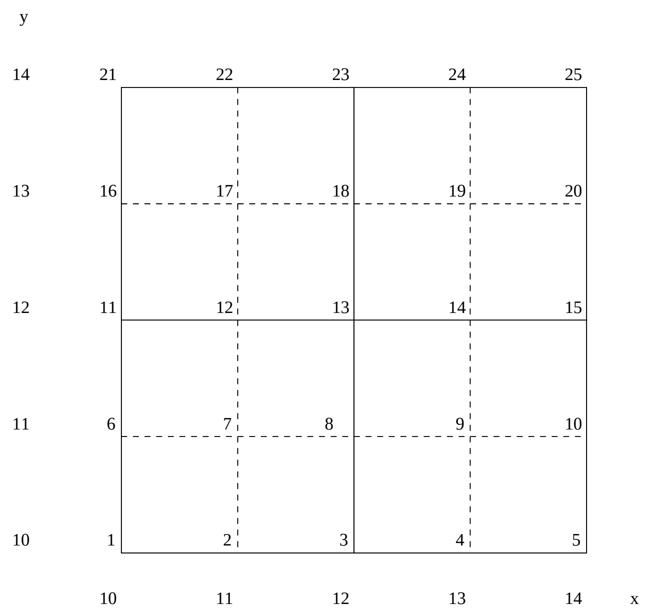

Figure 1. Node numbering for rectangular grid.

The test potentials are now given:
Example 1. $\phi = e^{ikx}$, $k = 2\pi$,
Example 2. $\phi = H_0(kr)$, $k = 2\pi$,
These shall be tested for various perturbations of the phase at nodes 12, 13 and 14 represented graphically.

We plot a graph at $y = 13$ along $10 \leq x \leq 14$ to see how the phase function s and the wave envelope A change with each iteration. We use 9-node Lagrange elements. Hence A and s are assumed to have quadratic variation within each element, and four elements are considered. We also plot the iterated value of the wave envelope and the potential.

For the plane wave $\phi = e^{ikx}$, consider perturbing node 12 by 0.2, node 13 by -0.4 and node 14 by 0.2, and running the program for ten iterations. (The sign of the perturbation for node 13 is chosen to be negative because the phase gradient then changes rapidly from node 12 to 14. This problem converges with more iterations than if the sign was positive because it is the phase gradient that is being determined in the element matrix integral and not the phase.) Figure 2 shows the plot of the initial estimate for the phase, and subsequent values of the phase for iterations 1, 3 and 10. From figure 6 we see that after ten iterations the exact value of the phase is obtained. (We note that although the value of the phase is a closer approximation for iteration 1 rather than iteration 3, the phase gradient varies more smoothly for iteration 3.)

In figure 3 we plot the corresponding values for the wave envelope. We see that after ten iterations the exact value of the wave envelope is obtained.

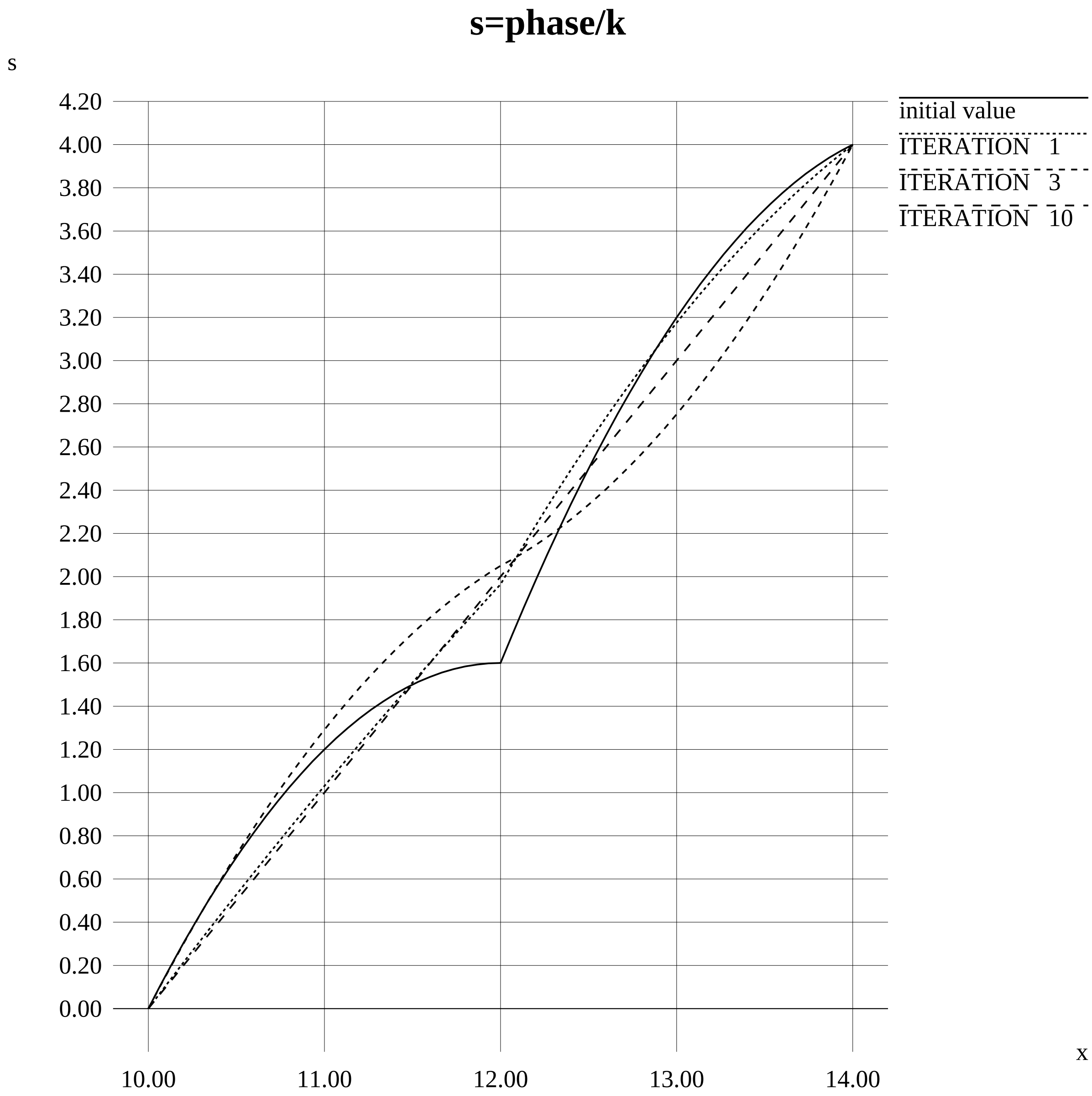

Figure 2. Example 1, cross-section along y=13. $k = 2\pi$, wavelength $= 1$.

A= Wave Envelope

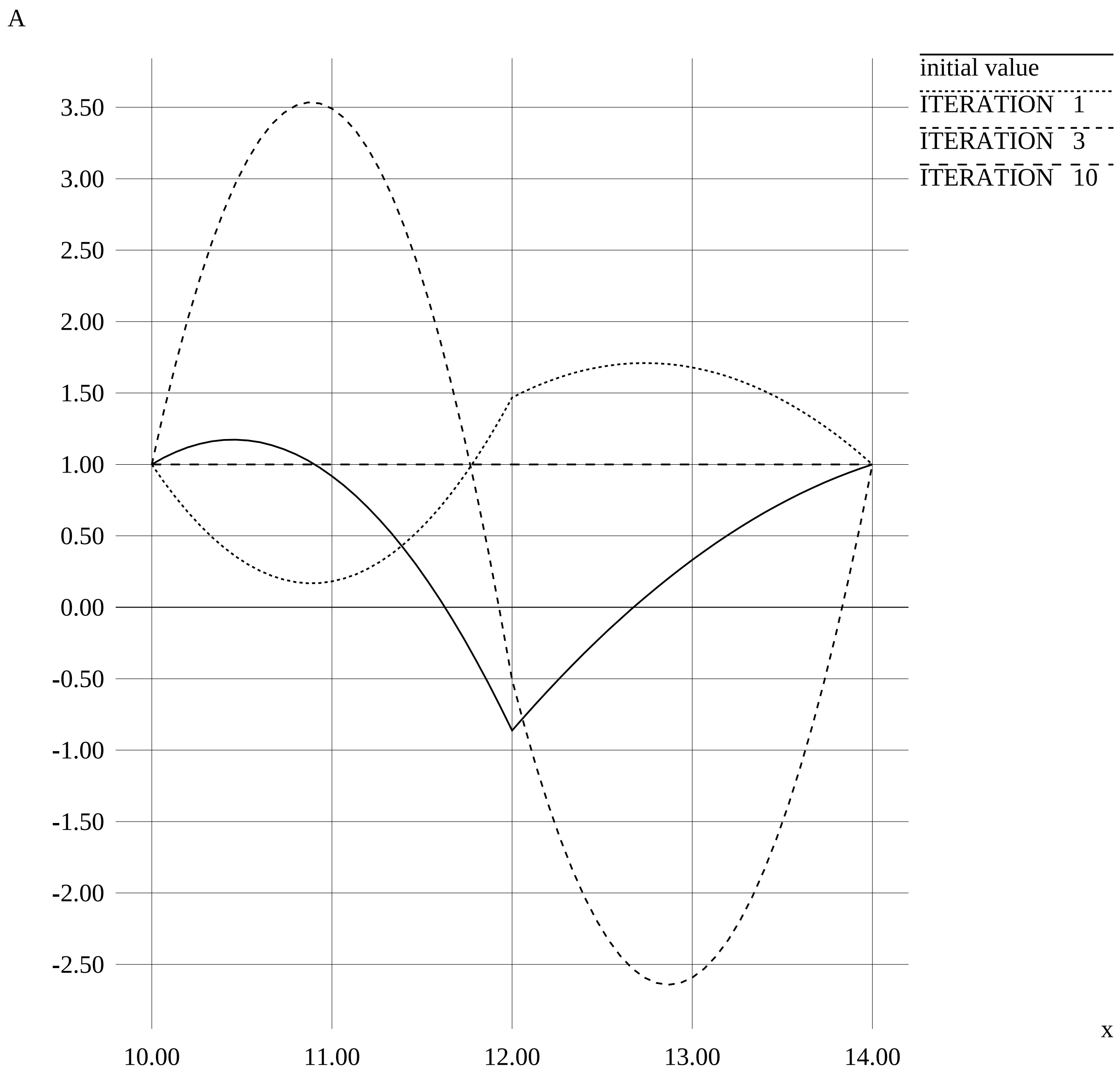

Figure 3. Example 1, cross-section along y=13. $k = 2\pi$, wavelength = 1.

We now consider the results for the Helmholtz source $H_0(kr)$, $k = 2\pi$ for example 2. In this example, we consider very large perturbations. We perturb the phase at node 12 by 1.0, node 13 by -2.0 and node 14 by 1.0. From figure 4 we find that after sixty iterations the exact value of the phase is obtained. In figure 5 the corresponding values for the wave envelope are plotted, and after sixty iterations the exact value of the wave envelope is obtained.

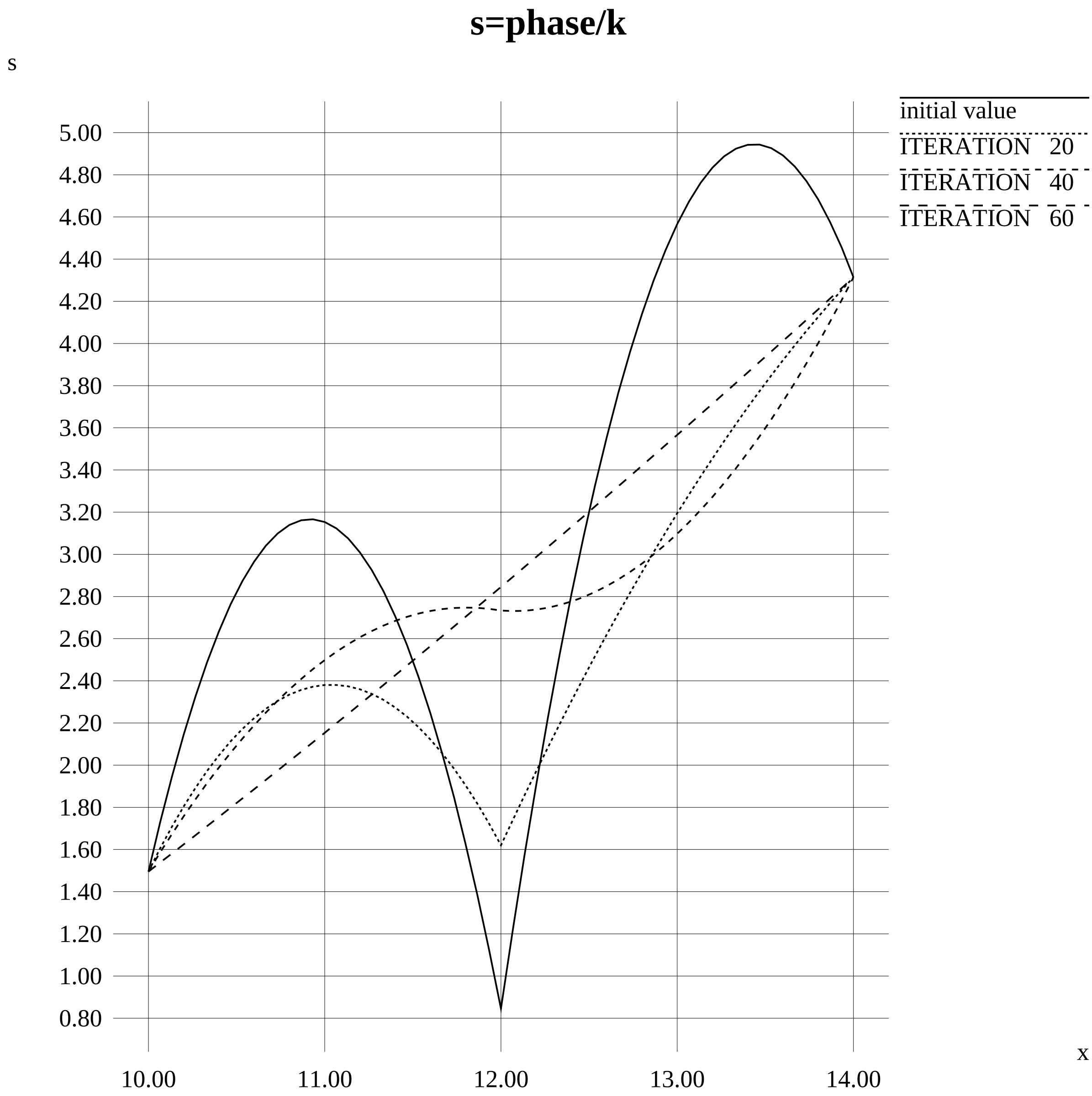

Figure 4. Example 2, cross-section along y=13. $k = 2\pi$, wavelength ~ 1.

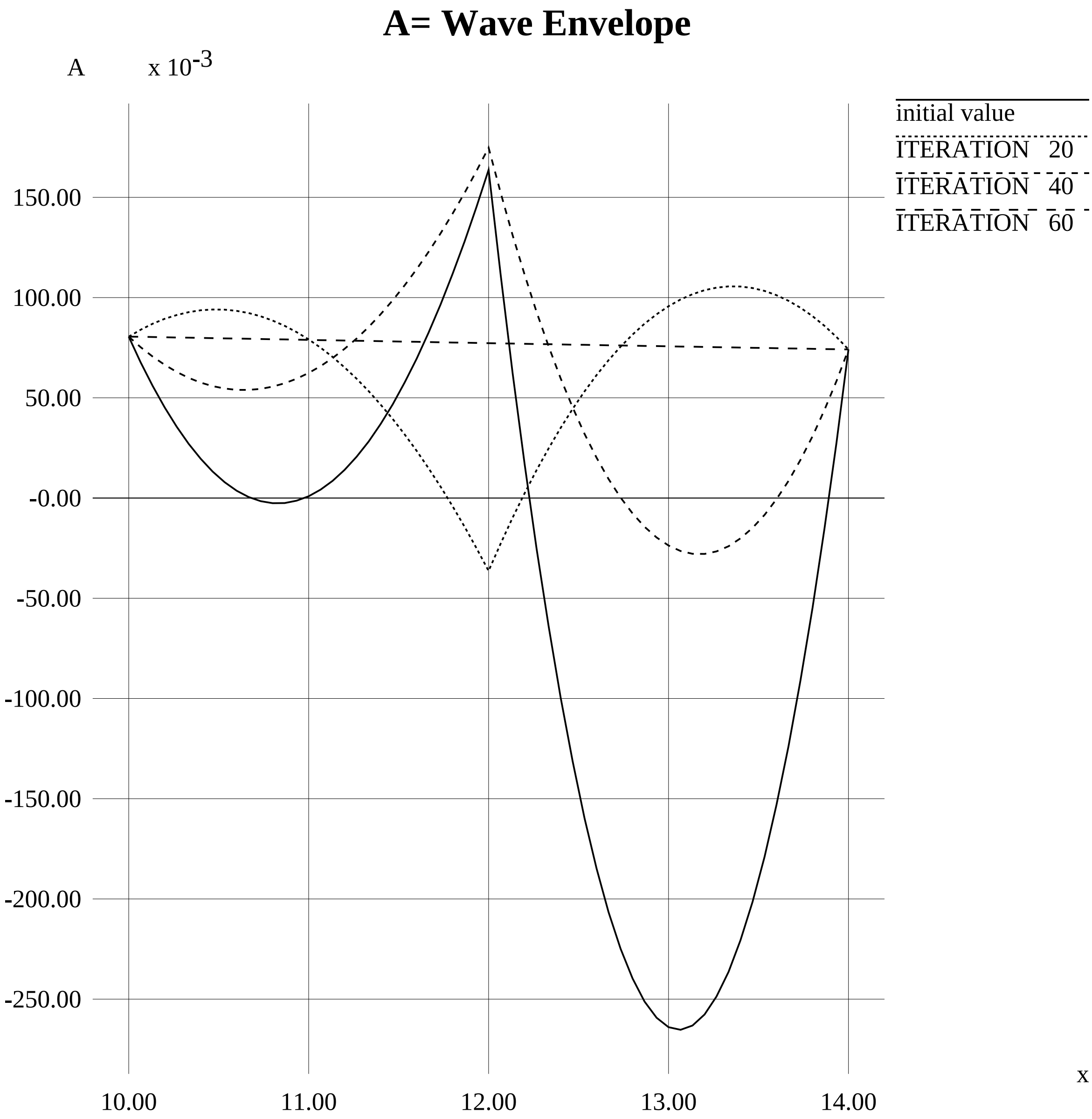

Figure 5. Example 2, cross-section along y=13. $k = 2\pi$, wavelength ~ 1.

The iterated values of the wave envelope A and the phase p are obtained within an element by interpolating from the nodal values of A and s using the nine node Lagrange element shape functions. Hence using (7) the potential is obtained within an element. Figure 6 shows the real part of the potential determined in this way. In figure 7, for comparison, the real part of the Hankel source function $H_0(kr)$ is plotted over the same domain. We see that the two plots are identical. Hence we have successfully obtained the potential after a poor initial estimate for the phase by using the iteration method.

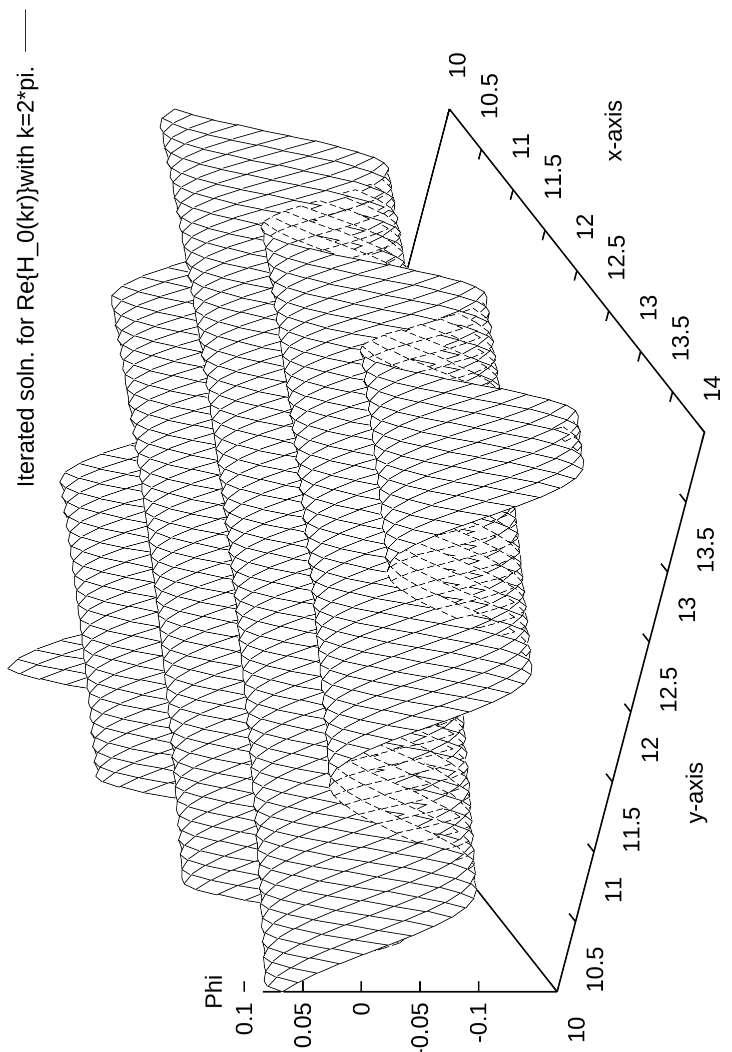

Figure 6. Example 2, iterated value of potential. $k = 2\pi$, wavelength ~ 1.

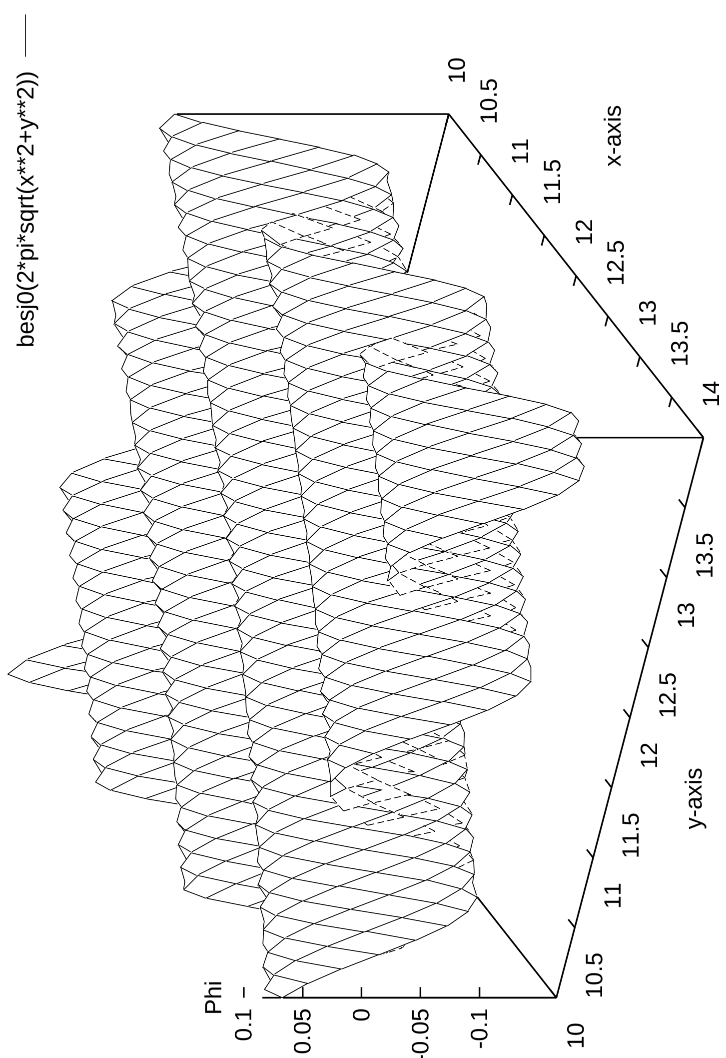

Figure 7. Example 2, exact value of potential. $k = 2\pi$, wavelength ~ 1.

3.2 Testing and comparing the two formulations.

In this subsection, we shall obtain an estimate for s by assuming that it varies linearly throughout the domain. Hence the initial guess for s is determined at all nodal points from the values of s at the constrained boundary nodes. The formulations are tested on the diffraction potential for plane waves incident upon a vertical cylinder.

The diffraction potential for example 3 is given by (20) as

$$\phi_D = -H_0(kr)\frac{J_0'(ka)}{H_0'(ka)} - \sum_{n=1}^{\infty} 2i^n \frac{J_n'(ka)}{H_n'(ka)} H_n(kr)\cos n\theta] \tag{21}$$

We consider a circular 5*5 grid of 25 evenly spaced nodes in the coordinates r and θ) in two regions, one in front of the cylinder and one behind the cylinder. The following problems are considered:
1. $\phi = \phi_D$, $a = 1$, $k = 2\pi$, $1 \le r \le 1.5$, $0 \le \theta \le \frac{\pi}{18}$
2. $\phi = \phi_D$, $a = 1$, $k = 20\pi$, $1 \le r \le 1.2$, $\frac{17\pi}{18} \le \theta \le \pi$

We consider the results for problem 1: 1. $\phi = \phi_D$, $a = 1$, $k = 2\pi$, $1 \le r \le 1.5$, $0 \le \theta \le \frac{\pi}{18}$

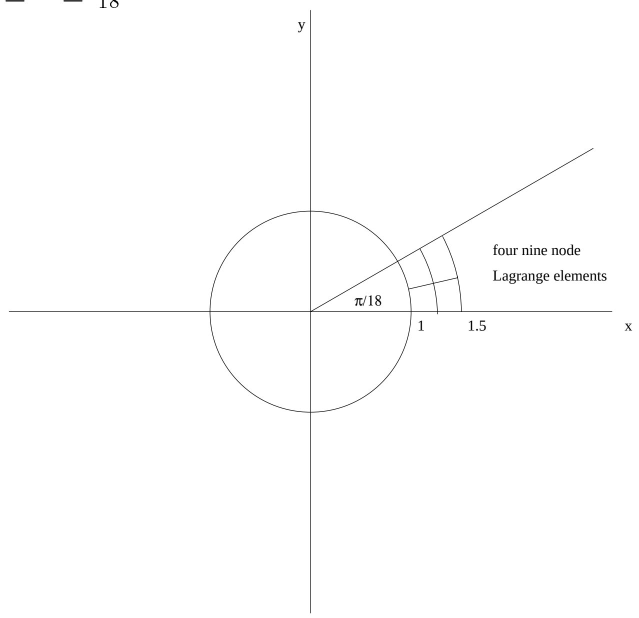

Figure 8. Domain for problem 1.

We run the program for ten iterations and plot the exact wave envelope, the wave envelope from the initial value of the phase, and the wave envelope after 1,3, and 10 iterations for the two formulations.

Considering figure 9, using the complete formulation, the exact value is obtained almost immediately and so very few iterations are necessary. However considering figure 10, using the generalized Astley formulation, we obtain an iterated value for the wave envelope after ten iterations but it is not the exact value.

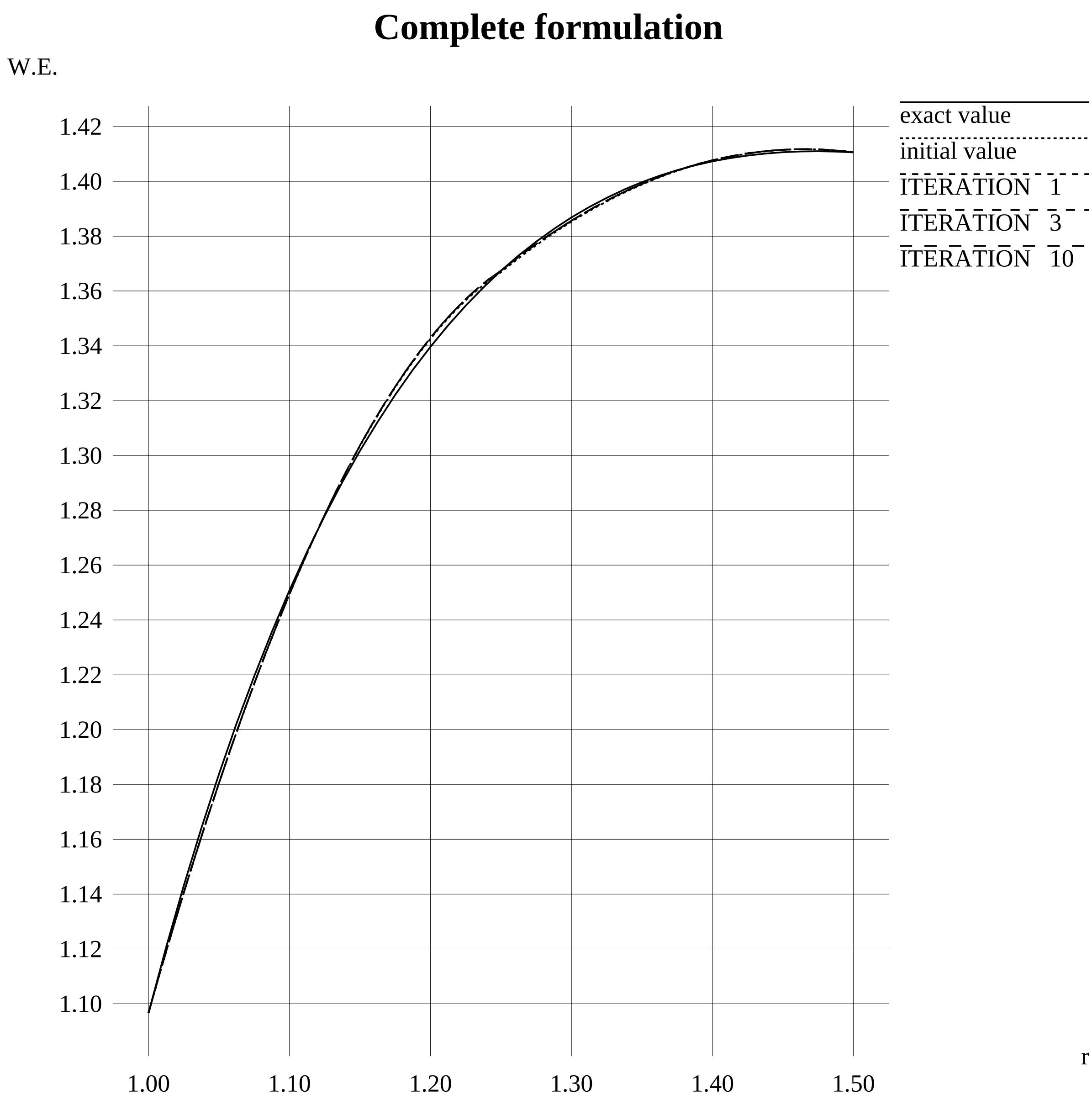

Figure 9. Example 3, cross-section along $\theta = \frac{\pi}{36}$ with complete formulation. $k = 2\pi$, wavelength ~ 1.

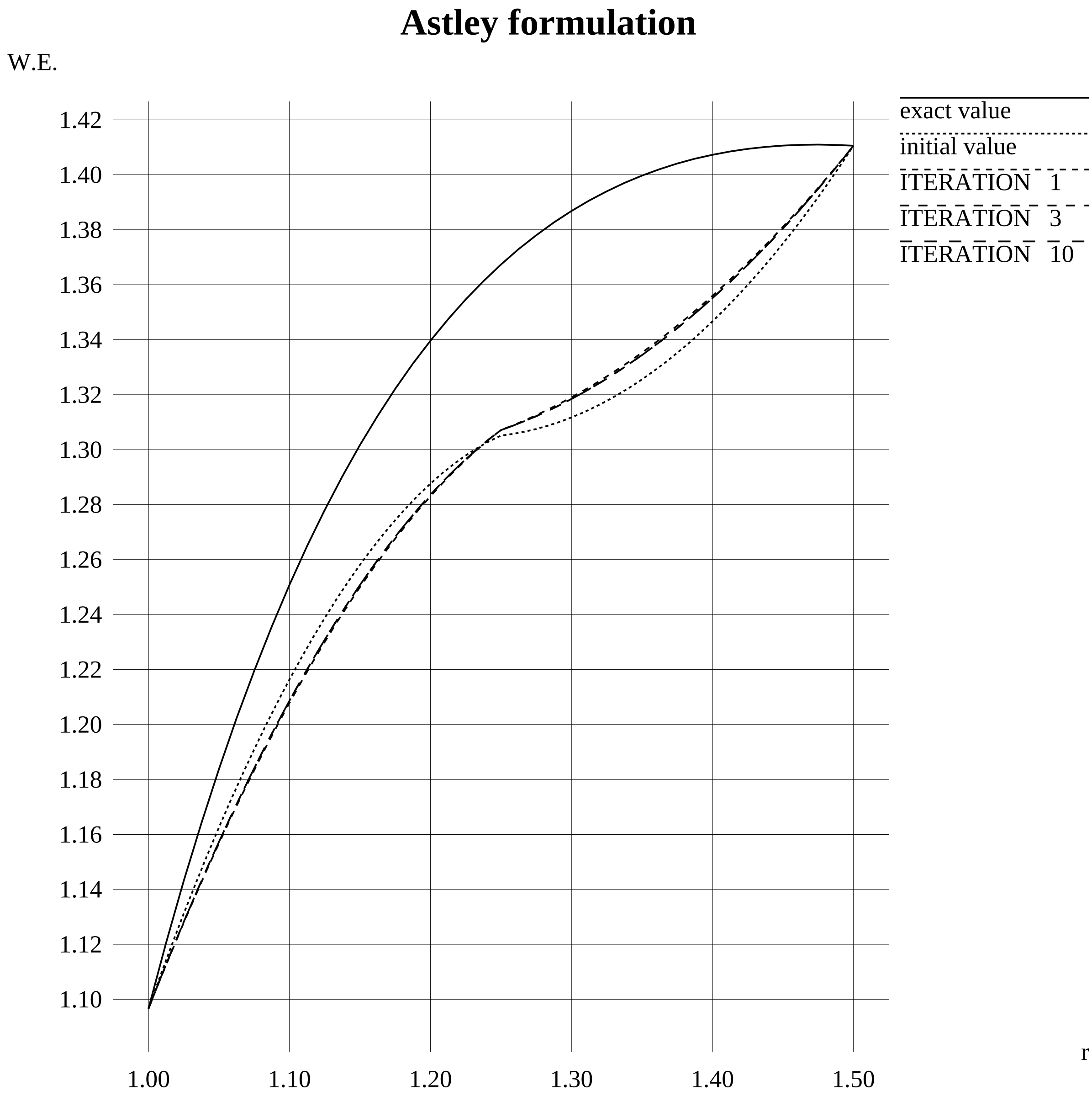

Figure 10. Example 3, cross-section along $\theta = \frac{\pi}{36}$ with generalised Astley formulation. $k = 2\pi$, wavelength ~ 1.

We consider the results for problem 2: 2. $\phi = \phi_D$, $a = 1$, $k = 20\pi$, $1 \leq r \leq 1.2$, $\frac{17\pi}{36} \leq \theta \leq \pi$

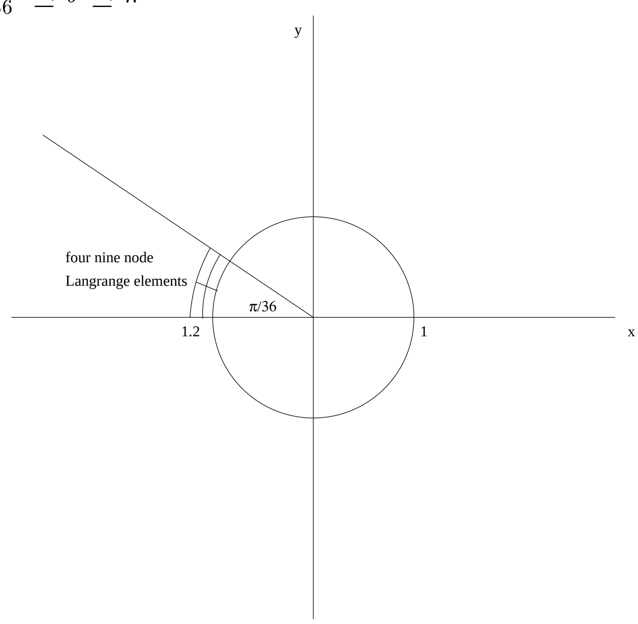

Figure 11. Domain for problem 2.

We run the program for ten iterations and plot the exact wave envelope, the wave envelope from the initial value of the phase, and the wave envelope after 1,3, and 10 iterations for the two formulations.

Considering figure 12, using the complete formulation the exact value is obtained almost immediately, and so very few iterations are necessary. However considering figure 13, using the generalized Astley formulation no convergent iterated solution for the wave envelope is obtained.

Thus for near field diffraction problems the generalized Astley formulation, in which the eikonal equaton is assumed valid, is not applicable even when the waves are short ($ka = 20\pi$). Hence the Astley formulation can only be used far from the body.

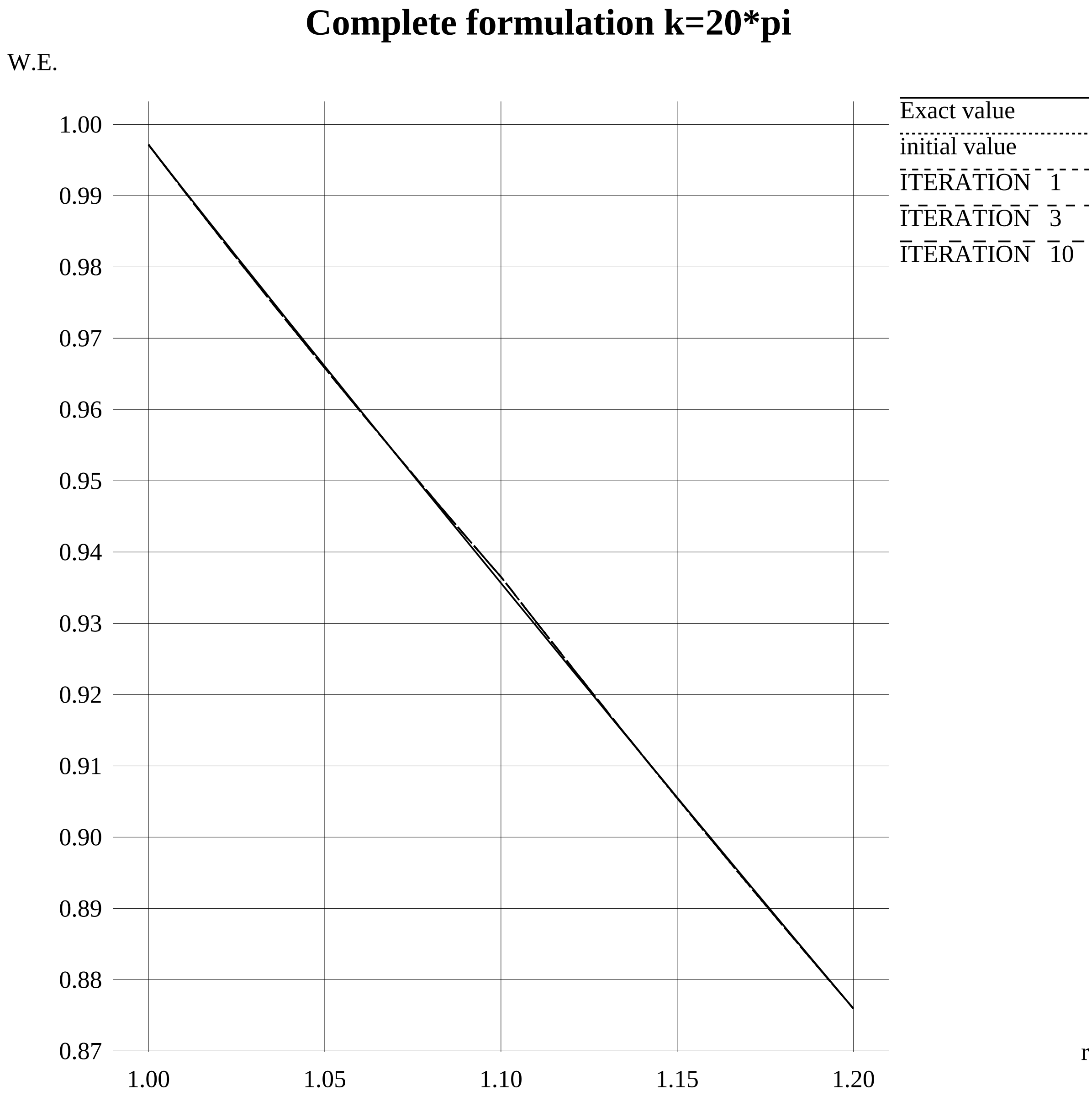

Figure 12. Example 3, cross-section along $\theta = \frac{35\pi}{36}$ with complete formulation. $k = 20\pi$, wavelength ~ 0.1.

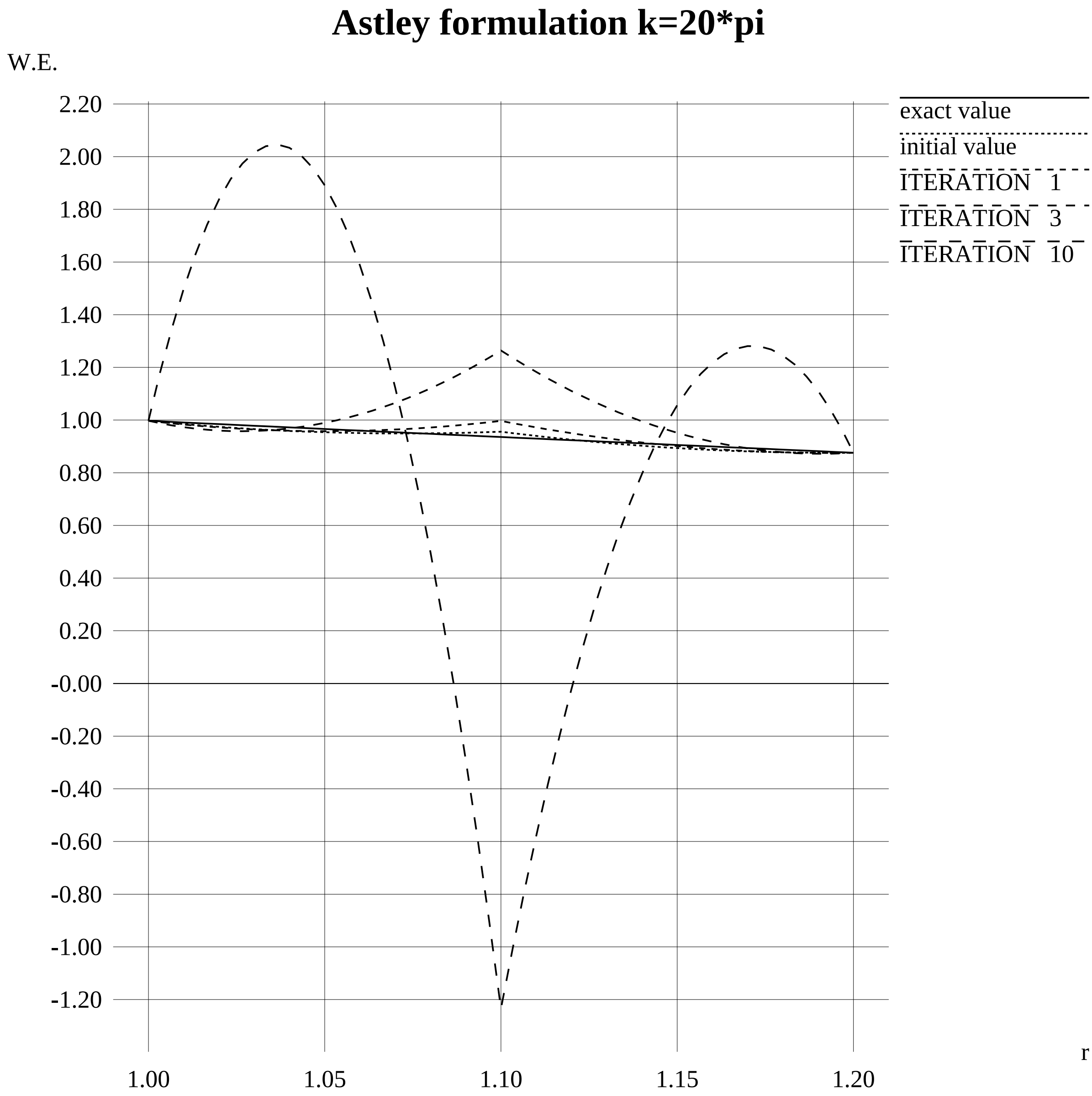

Figure 13. Example 3, cross-section along $\theta = \frac{35\pi}{36}$ with generalised Astley formulation. $k = 20\pi$, wavelength ~ 0.1.

The iterated values of the wave envelope A and the phase p are obtained within an element by interpolating from the nodal values of A and s using the nine node Lagrange element shape functions. Hence using (7) the potential is obtained within an element. Figure 14 shows the real part of the potential determined in this way. In figure 15, for comparison, the real part of the diffracton potential given by (21) is plotted over the same domain. We see that the two plots are identical. Hence we have successfully obtained the potential using the complete formulation. We note, refering to figs. 14 and 15 that we have pure reflection at the front of the cylinder, giving a total amplitiude of 2 from the incident and diffracted waves.

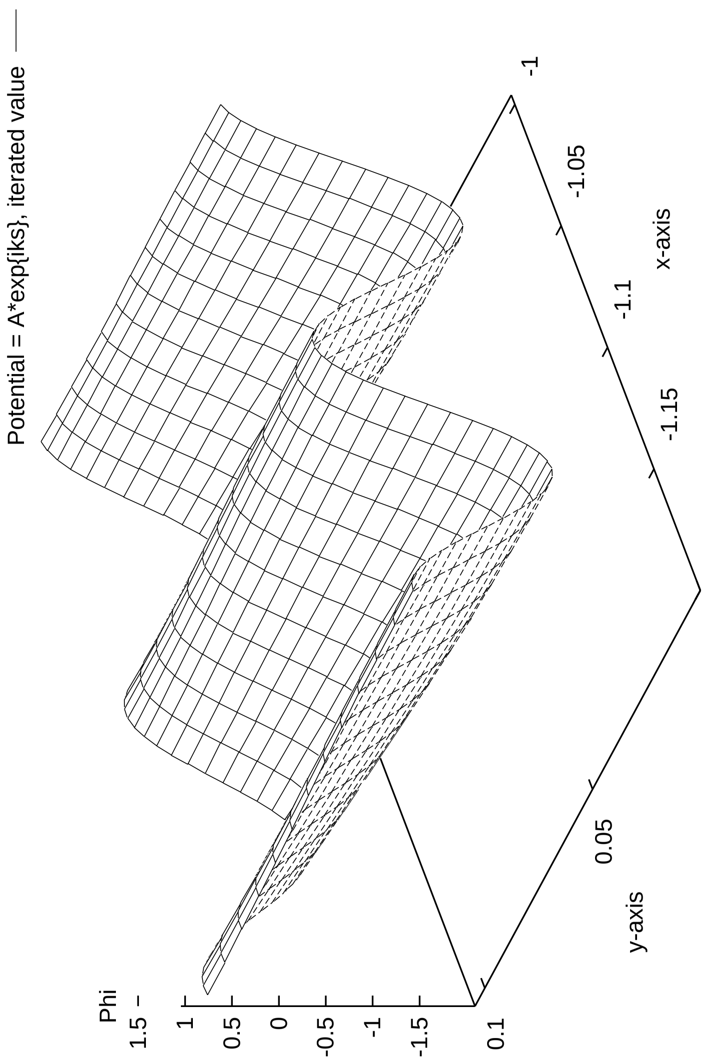

Figure 14. Example 3, iterated value for potential, complete formulation. $k = 20\pi$, wavelength ~ 0.1.

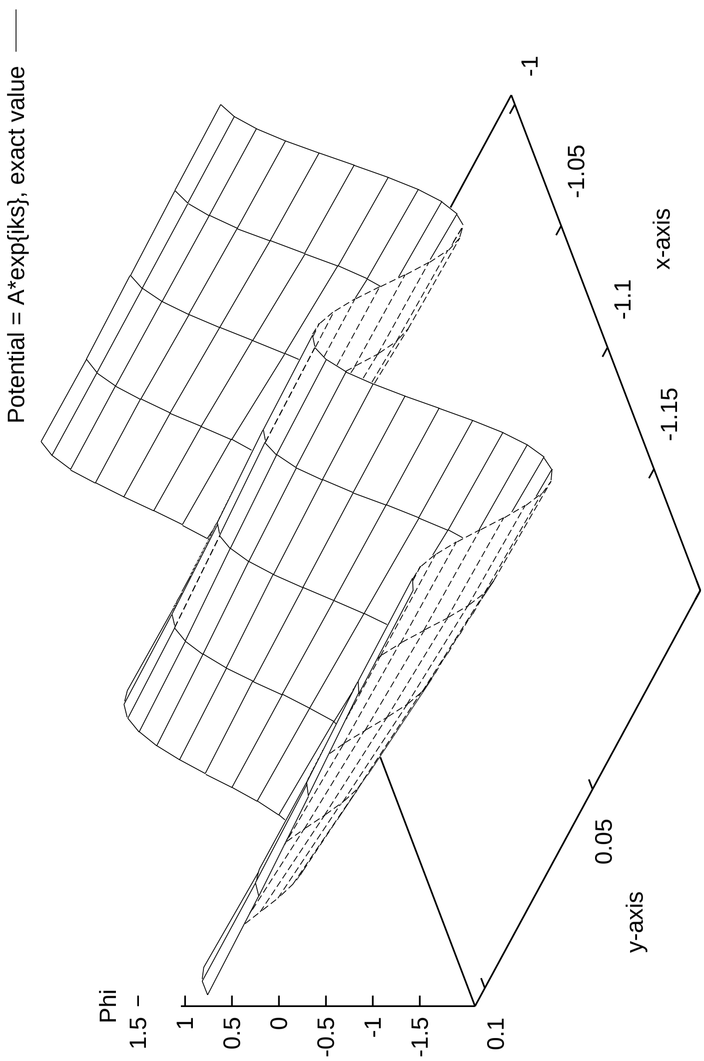

Figure 15. Example 3, exact value for potential. $k = 20\pi$, wavelength ~ 0.1.

4 Conclusion.

The method holds great promise. It is the only finite element model known to the authors which has the capability to solve problems where the wavelength is much smaller than the element size.

The iteration method has proved to be successful; when the phase was perturbed at unconstrained nodes within the domain, the iterated values for the phase and wave envelope yielded the expected solution for the progressive waves e^{ikx} and $H_0(kr)$. We find that without exception the method always converges, although if a very poor estimate for the phase is first given the iterated values converge very slowly. Thus a method to accelerate convergence, by considering the trend of the values over a few iterations, would be of great use. However, from fig. 5 we see that convergence is strongly non-uniform, making determining any trend difficult. This problem will have to be looked at in greater detail.

For the diffraction potential with $ka = 2\pi$ and $ka = 20\pi$, a is the cylinder radius, it is found that in the near field domain the 'complete formulation' proved better than the 'generalised Astley formulation'. Hence it seems better not to assume the eikonal equation holds near the cylinder.

The present paper provides a test for a method which it is hoped to use on diffraction problems. This test has proved successful and so future work involves solving a diffraction problem, in particular short wave diffraction past a cylinder. One future difficulty will be the choice for the estimate for the phase function in order to reduce the number of iterations. Also, as $ka \to \infty$, the amplitude varies rapidly in the 'shadow region' $|y| < a$, $x > 0$.

REFERENCES

1. M. Born and E.Wolf, *Principles of Optics: Electromagnetic Theory of Propagation, Interference and Diffraction of Light*, (Pergamon Press; Oxford 5th edn, 1975)

2. F.B. Jensen, W.A. Kuperman, M.B. Porter, H. Schmidt, *Computational Ocean Acoustics*, (American Institute of Physics; New York 1994)

3. J.B. Keller, 'Geometrical theory of diffraction', *Jour. Opt. Doc. Am.* **52**, 116 (1962)

4. P. Bettess, E.A. Chadwick, 'Wave envelope examples for progressive waves', *Comm. Num. Meth. Eng.* (1995).

5. O.C. Zienkiewicz, P. Bettess, 'Infinite elements in the study of fluid-structure interaction problems', *Computing methods in Applied Sciences, Lecture notes in Physics, Springer-Verlag, Berlin* **58**, 133-169 (1975).

6. P. Bettess , O.C. Zienkiewicz, 'Diffraction and refraction of surface waves using finite and infinite elements', *Int. Jour. Num. Meth. Eng.* **11**, 1271-1290 (1977).

7. R.J.Astley, 'Wave envelope and infinite elements for acoustical radiation', *Int. Jour. Num. Meth. Fluids,* **3**, 507-526 (1983).

8. R.J. Astley and W. Eversman, 'Finite element formulation for acoustical radiation', *Jour. Sound and Vib.* **88(1)**, 47-64 (1983).

9. R.J. Astley and G.J. Macaulay and J.P. Coyette, 'Mapped wave envelope elements for acoustical radiation and scattering', *Jour. Sound and Vib.* **170(1)**, 97-118 (1994).

10. E.H. Thompson, *An introduction to the algebra of matrices with some applications*, (Adam Hilger Ltd; London, 1969)

11. O.C. Zienkiewicz and R.L. Taylor, *The Finite Element Method, 4th edn. Vol. 1* (McGrawHill; London, 1989)

12. H. Lamb, *Hydrodynamics* (Cambridge University Press 1932)

13. P.C. Etter, *Underwater Acoustic Modeling: Principles, Techniques and Application*, (Elsevier Science Publishers; New York, 1991)

14. P. Bettess, *Infinite Elements*, (Penshaw Press; The Lawns, Undercliff, Cleadon Lane, Cleadon, Sunderland, U.K., 1992)

15. A.M. Abramowitz and I.N. Stegun, *Handbook of Mathematical Functions* (Dover; New York, 1965)

16. R.C. MacCamay and R.A. Fuchs, 'Wave Forces on Piles. A Diffraction

Theory', *Beach Erosion Board Tech. Mem. No. 69* (1954).
17. T.H. Havelock, 'The pressure of water waves upon a fixed obstacle', *Proc. Roy. Soc. Lon., Series A* No. 963 **175**, 409-421 (1940)

Appendix A

To show that the $n * n$ skew symmetric matrix where n is odd has zero determinant.

We may represent the determinant D of the matrix a_{ij} by

$$D = \begin{vmatrix} 0 & a_{12} & a_{13} & ... & a_{1n} \\ -a_{12} & 0 & a_{23} & ... & a_{2n} \\ -a_{13} & -a_{23} & 0 & ... & a_{3n} \\ ... & ... & ... & ... & ... \\ -a_{1n} & -a_{2n} & 0 & ... & 0 \end{vmatrix} \tag{22}$$

where $1 \leq i, j, \leq n$, n odd. We may multiply each column in the determinant expression by -1. Since there are an odd number of rows, then from [16, p36]

$$-D = \begin{vmatrix} 0 & -a_{12} & -a_{13} & ... & -a_{1n} \\ a_{12} & 0 & -a_{23} & ... & -a_{2n} \\ a_{13} & a_{23} & 0 & ... & -a_{3n} \\ ... & ... & ... & ... & ... \\ a_{1n} & a_{2n} & 0 & ... & 0 \end{vmatrix} \tag{23}$$

This is the determinant of the transpose. However, from [16,p35] the determinant of the transpose of a matrix is equal to the determinant of the matrix itself. Hence $D = 0$.

Appendix B

We want to give s and A at 'boundary nodes' (nodes on the boundary enclosing the domain) given the potential ϕ on the boundary where

$$\phi = Ae^{iks} \tag{24}$$

Hence

$$A = |\phi| \tag{25}$$

$$ks = -i\ln\{\frac{\phi}{|\phi|}\} + 2\pi n$$

where is an integer value step function dependent upon position on the boundary. There is a difficulty in determining ks because the function $-i\ln\{\frac{\phi}{|\phi|}\}$ is always given in the principal value range $-\pi < -i\ln\{\frac{\phi}{|\phi|}\} < \pi$ and so n is an unknown. However, we want ks to be a continuous function with no discontinuous 'jumps' in 2π. This criterion for ks gives us a method for determining n at each nodal point on the boundary, and hence for determining ks from (18). The method is described below. We divide the boundary contour between 'boundary nodes' into length intervals L of approxmately $\frac{1}{10}$ of a wavelength of the wave disturbance. Hence we let

$$L = \frac{2\pi}{10k} \tag{26}$$

where k is the wavenumber. We assume ks is known at the first boundary node $\underline{x_1}$ but not known at the second boundary node $\underline{x_2}$. From the first boundary node, we move a distance L along the boundary and determine the value $-i\ln\{\frac{\phi}{|\phi|}\}$ which is compare with its value at node $\underline{x_1}$. If

$$\left[-i\ln\{\frac{\phi}{|\phi|}\}\right]_{\underline{x_1}}^{\underline{x_1}+\underline{L}} \sim 2\pi$$

then n has decreased by one from $\underline{x_1}$ to $\underline{x_1} + \underline{L}$. If

$$\left[-i\ln\{\frac{\phi}{|\phi|}\}\right]_{\underline{x_1}}^{\underline{x_1}+\underline{L}} \sim -2\pi$$

then n has increased by one from $\underline{x_1}$ to $\underline{x_1} + \underline{L}$, and if

$$\left[-i\ln\{\frac{\phi}{|\phi|}\}\right]_{\underline{x_1}}^{\underline{x_1}+\underline{L}} \sim 0(\frac{2\pi}{10})$$

then n remains the same value. Hence the following algorithm can be employed:
if $\left[-i\ln\{\frac{\phi}{|\phi|}\}\right]_{\underline{x_1}}^{\underline{x_1}+\underline{L}} > \pi, \quad n_{\underline{x_1}+\underline{L}} = n_{\underline{x_1}} - 1$
if $\left[-i\ln\{\frac{\phi}{|\phi|}\}\right]_{\underline{x_1}}^{\underline{x_1}+\underline{L}} < -\pi, \quad n_{\underline{x_1}+\underline{L}} = n_{\underline{x_1}} + 1$
otherwise, $n_{\underline{x_1}+\underline{L}} = n_{\underline{x_1}}$
This is repeated for each interval step L along the boundary. Hence the value of ks at the second boundary node $\underline{x_2}$ is determined.